NI MHD Modeling of the Corona and Turbulence

Laxman Adhikari[1], Gary Zank[1], Lingling Zhao[1], and Daniele Telloni[2]

[1]Department of Space Science and Center for Space Plasma and Aeronomic Research

[2]INAF, Torino, Italy

First meeting, ISSI, December 5 – 9, 2022

Temperature of the solar corona

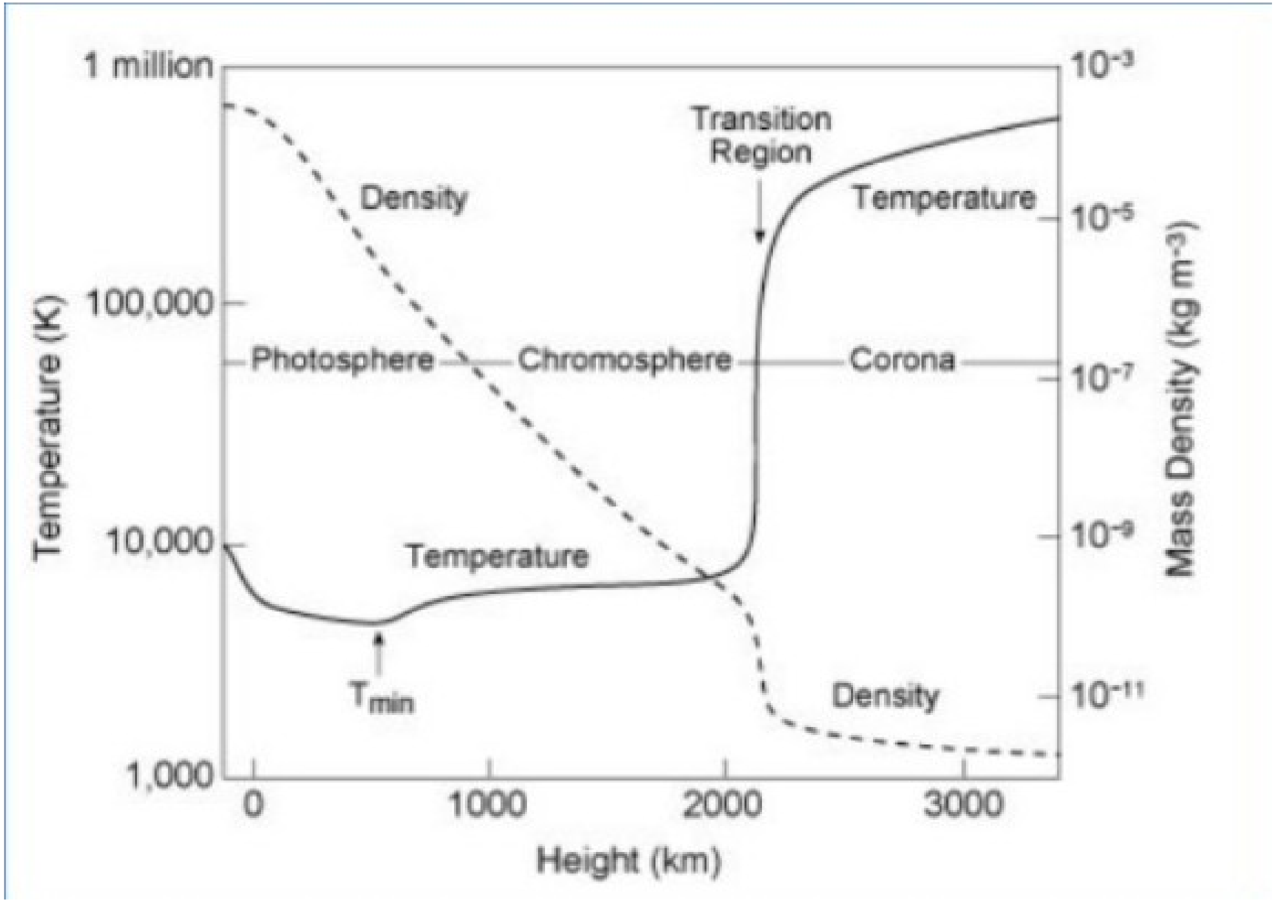

Wave/Turbulence approach

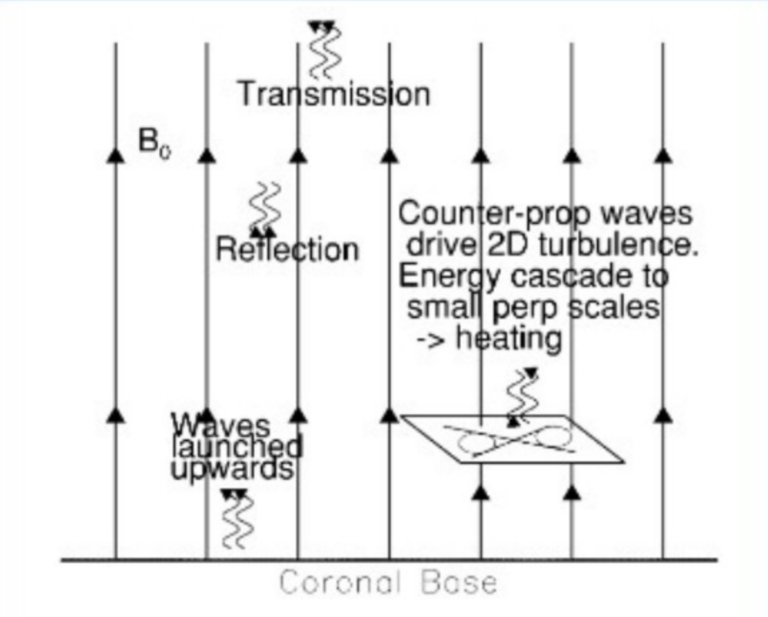

FIG. 1.—Cartoon sketch of the basic physics underlying the proposed coronal heating mechanism.

(Matthaeus et al 1999)

Lee/Donahue/Chandran

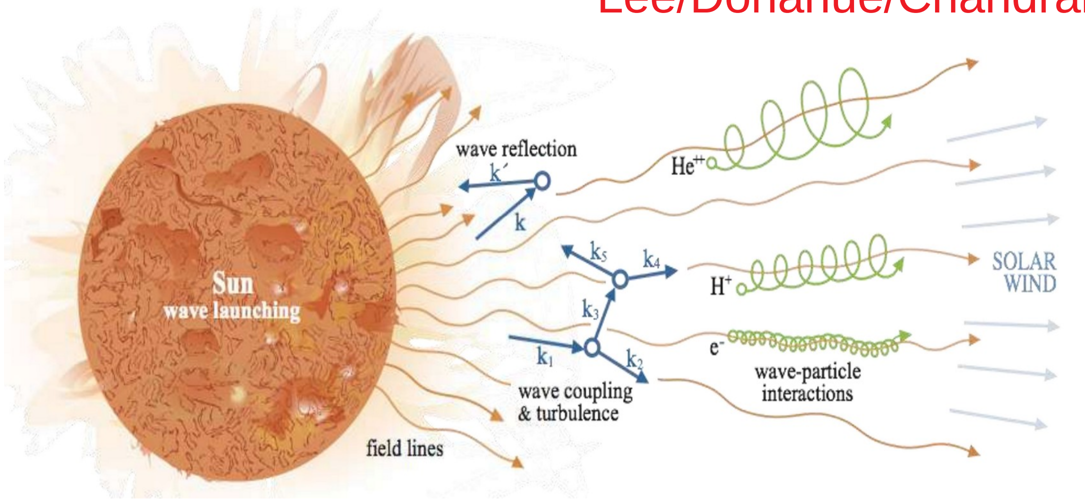

Many papers followed Matthaeus et al 1999 approach (e.g., Matsumoto & Shibata 2010; Verdini et al. 2010; Chandran et al. 2011; Lionello et al. 2014; Woolsey & Cranmer 2014)

Reconnection/Loop opening approach

Transverse photospheric motions lead to "twisting and braiding" of magnetic field lines and energy released in form of current sheets, with dissipation thought to occur via nanoflares (Parker, 1972, 1988, 1994)

- Mass and energy deposited into open-field regions via interchange reconnection (Fisk et al., 1999, Fisk, 2003)
- Magnetic carpet (Title & Schrijver, 1998) - photosphere

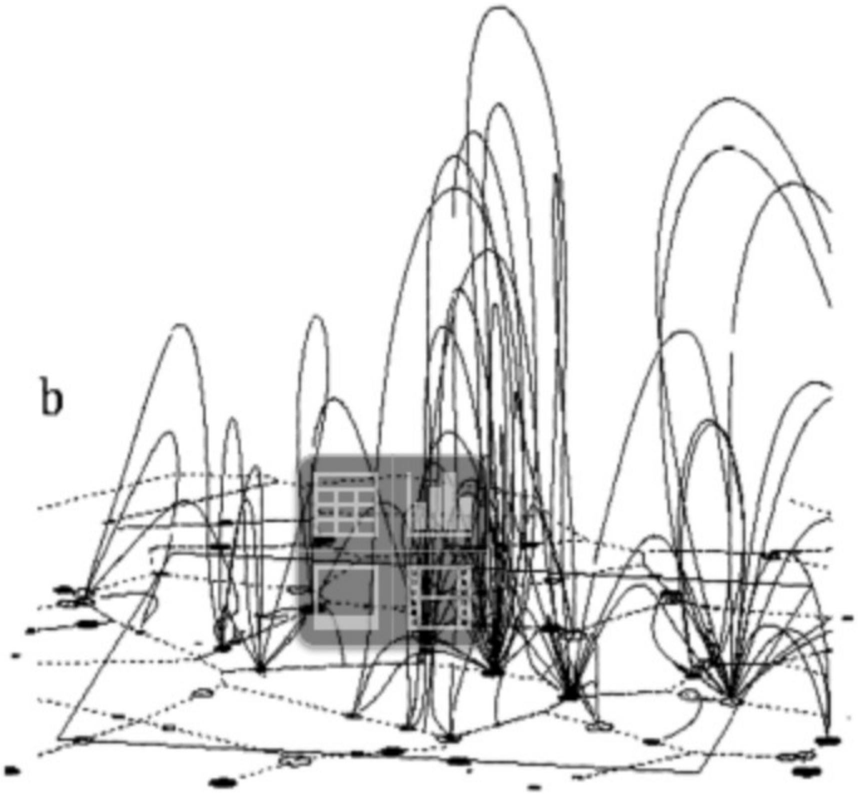

Generation of 2D turbulence

Closely related to the ideas of Parker (1972, 1988, 1994); Fisk 2003, Fisk et al 1999).

(Rappazzo and Parker 2013)

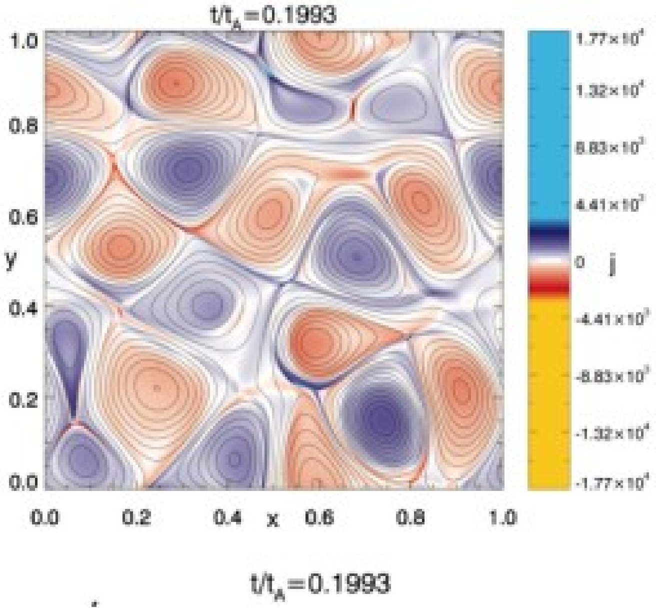

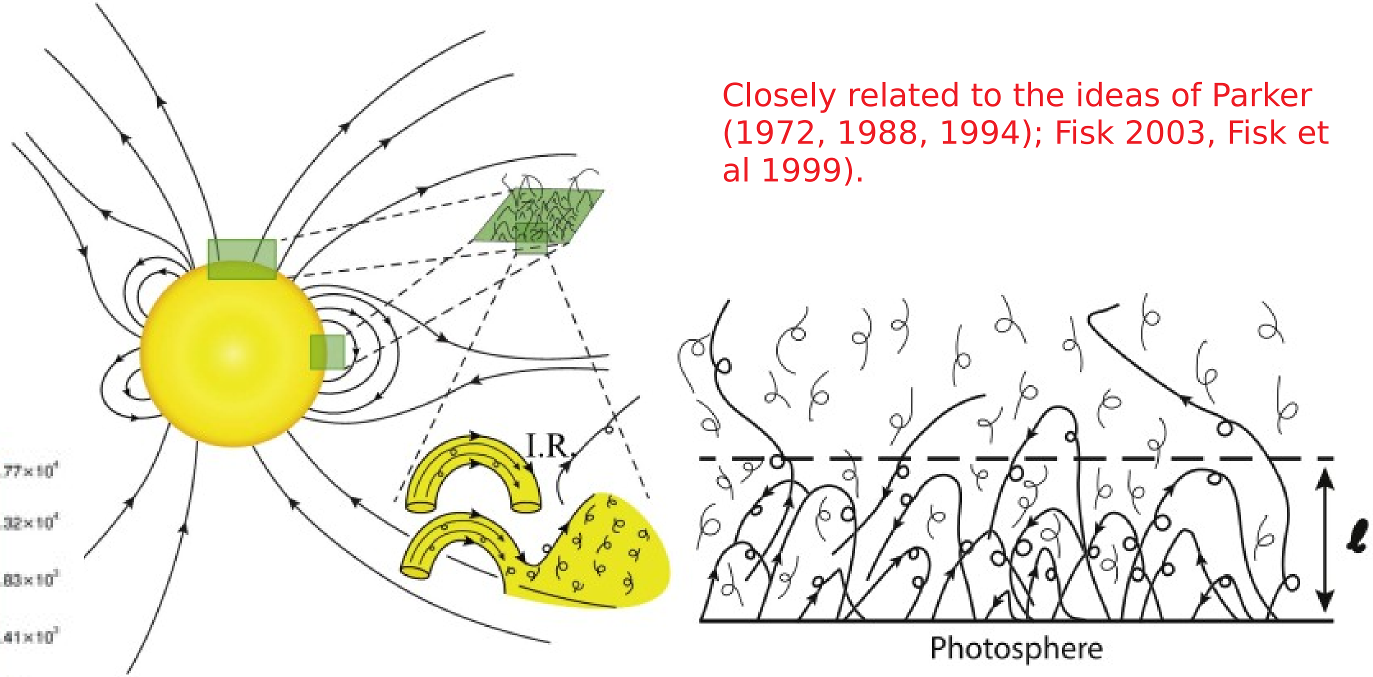

(Zank et al 2018)

2D+slab vs W/T transport model of coronal turbulence

NI 2D+slab model

- Majority 2D and minority slab in energy-containing range
- Anisotropic IR, primarily 2D, minority slab
- Uni-directional Alfven/slab propagation with $k_{||}^{-5/3}$ spectra is possible
- O(M) density fluctuations, $k_p^{-5/3}$ spectra, and variance

W/T model

- Majority slab and minority 2D in energy containing range
- Either isotropic IR likely or G-S scaling
- Uni-directional Alfven/slab propagation with $k_{||}^{-5/3}$ spectra is not possible
- O(M) density fluctuations

- 2D turbulence and NI/slab turbulence follow the ordering M_A^t : (M_A^t)^2 (Zank et al 2017), where M_A^t is the turbulent Alfven Mach number.

The Astrophysical Journal, 876:26 (12pp), 2019 May 1
https://doi.org/10.3847/1538-4357/ab141c

Does Turbulence Turn off at the Alfvén Critical Surface?

L. Adhikari[1], G. P. Zank[1,2], and L.-L. Zhao[1]
[1] Center for Space Plasma and Aeronomic Research (CSPAR), University of Alabama in Huntsville, Huntsville, AL 35899, USA
[2] Department of Space Science, University of Alabama in Huntsville, Huntsville, AL 35899, USA
Received 2018 November 13; revised 2019 February 11; accepted 2019 March 26; published 2019 April 30

NI 2D+slab model

$$\sigma_c^* = \pm 1, \ \sigma_D^* = 0, \ E_T^* \text{ arbitrary},$$

$$L^* \text{ arbitrary}, \ \text{and } L_D^* \text{ arbitrary},$$

$$\sigma_c^\infty \neq \pm 1, \ \sigma_D^\infty \neq 0, \ E_T^\infty \text{ arbitrary},$$

$$L_\infty^\pm \text{ arbitrary}, \ \text{and } L_D^\infty \text{ arbitrary}.$$

$$\boldsymbol{NL}_\pm^{\mathrm{Total}} = -z^{\infty\pm} \frac{E_T^{\infty 1/2}|1 \mp \sigma_c^\infty|^{1/2}}{\lambda_\infty^\pm} - z^{*\pm} \frac{E_T^{\infty 1/2}|1 \mp \sigma_c^\infty|^{1/2}}{\lambda_\infty^\pm} \neq 0.$$

Nonlinear dissipation term

- Turbulence does not turn off at the Alfven critical surface/highly field-aligned flow

W/T model

$$\sigma_c = -1, \ \sigma_D \text{ arbitrary}, \ E_T \text{ arbitrary},$$

$$L^+ = 0, \ L^- \text{ arbitrary}, \ \text{and } L_D \text{ arbitrary}$$

Nonlinear dissipation term

$$\boldsymbol{NL}_\pm = 0 \quad \text{and} \quad NL_{\mathrm{diss}}^{\mathrm{Total}} = 0.$$

- Turbulence turns off at the Alfven critical surface/highly field-aligned flow

(See also Alberti et al 2022)

NI MHD Coronal Turbulence Model

Fixed background profile

$$\mathbf{U} = U_0\left(\frac{r}{r_0}\right)\hat{r} \quad \rho = \rho_0\left(\frac{r_0}{r}\right)^3 \quad \mathbf{B} = B_0\left(\frac{r_0}{r}\right)^2\hat{r}$$

$$\mathbf{V}_A = \frac{\mathbf{B}}{\sqrt{\mu_0\rho}} = \frac{B_0}{\sqrt{\mu_0\rho_0}}\left(\frac{r_0}{r}\right)^{1/2}\hat{r} = V_{A0}\left(\frac{r_0}{r}\right)^{1/2}\hat{r}$$

where U_0 = 30 km/s and V_{A0} = 900 km/s

➡ Alfven surface ~ 11.69 Rsun

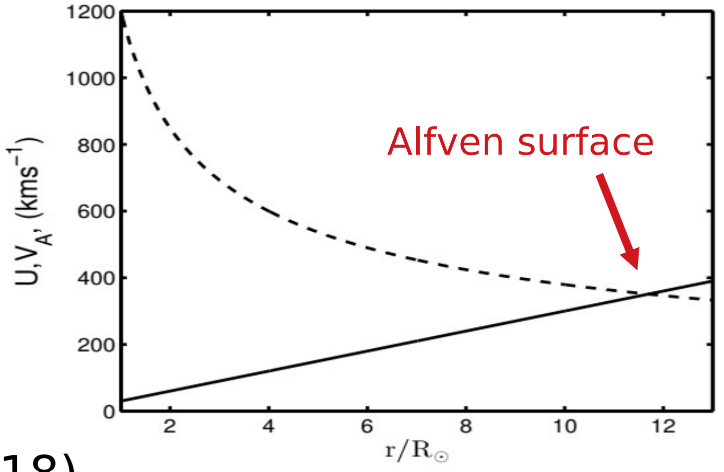

(Zank et al 2018)

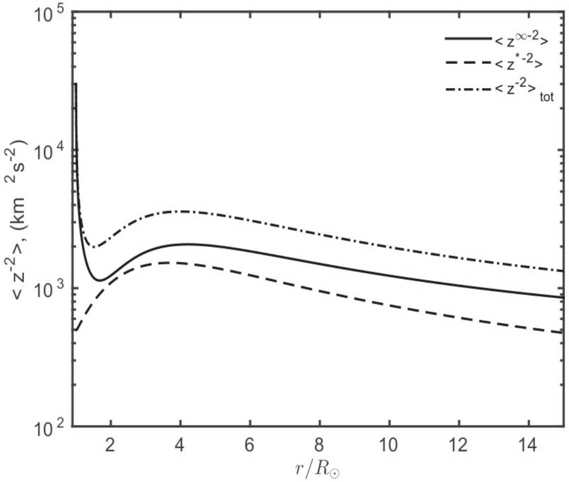

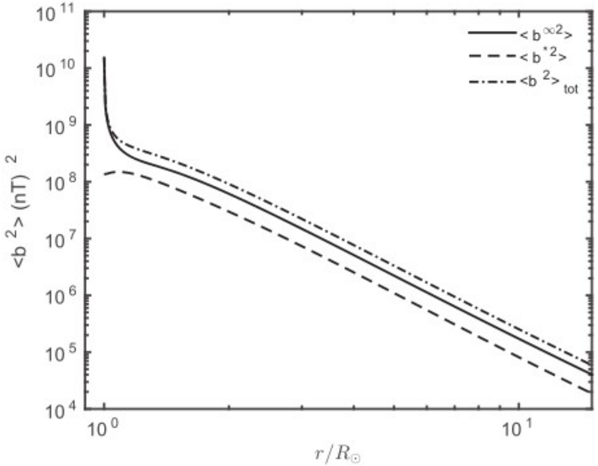

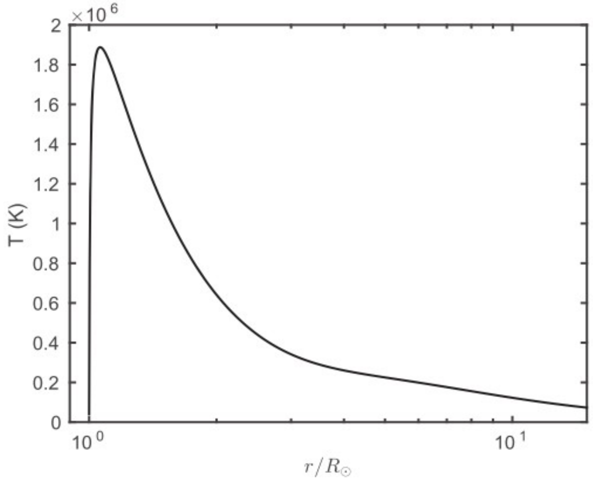

Structures in the solar atmosphere

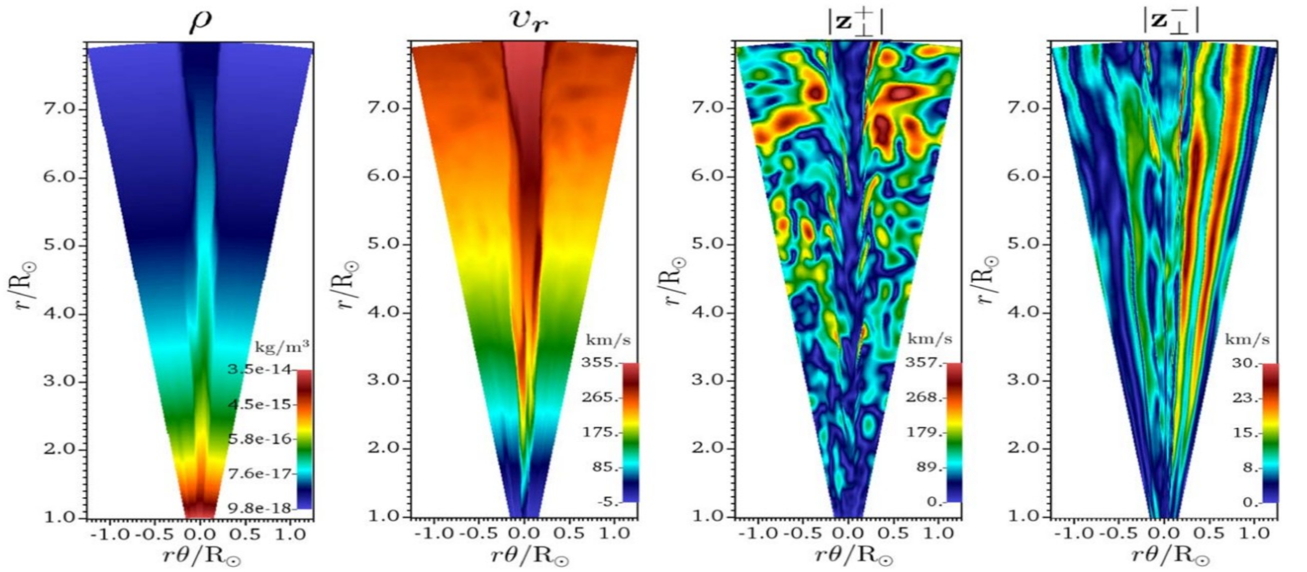

Figure 14. Snapshots of density (ρ), radial velocity (v_r), and the perpendicular Elsässer variables $|z_\perp^+|$ and $|z_\perp^-|$, respectively (from left to right), in a slice at $\phi = \pi/2$, 1 t_A after the start of the simulation, in the stochastically driven plume simulation.

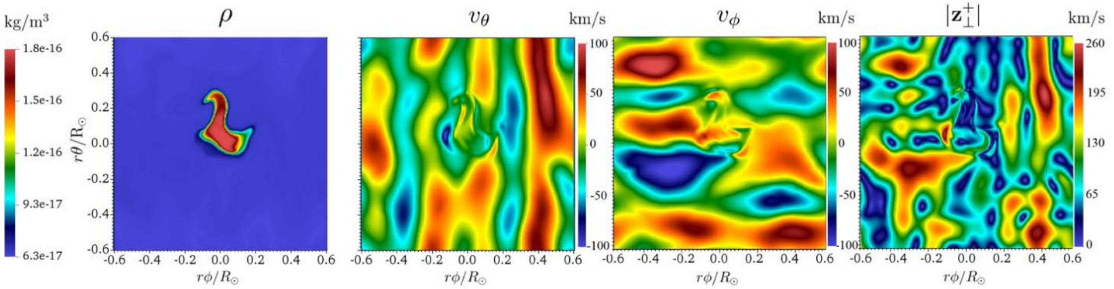

Figure 15. Snapshots of density (ρ), perpendicular velocity components (v_θ and v_ϕ), and the perpendicular Elsässer variable $|z_\perp^+|$, respectively (from left to right), in a spherical slice at $r = 4\ R_\odot$, 1.5 t_A after the start of the simulation, in the stochastically driven plume simulation.

(Magyor et al 2021)

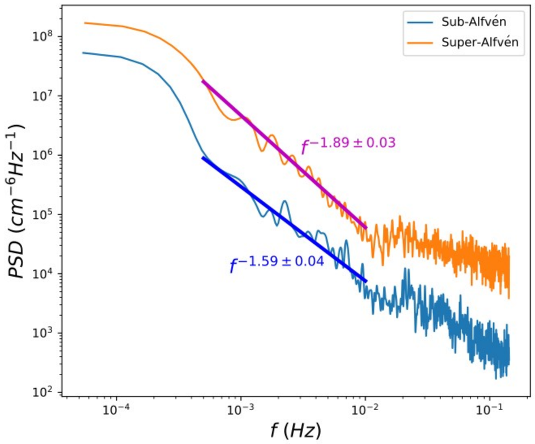

- Spacecraft cannot measure the 2D turbulence in the parallel geometry between the background fields. This does not mean that 2D turbulence is absent.
- The entropic density fluctuations are advected by the dominant 2D velocity fluctuations in the sub- and super-Alfvenic region during encounter 8 (where the background fields are parallel, and PSP observes only the slab component), consistent with the NI MHD description.

(Zank et al 2022)

Structures near the Sun

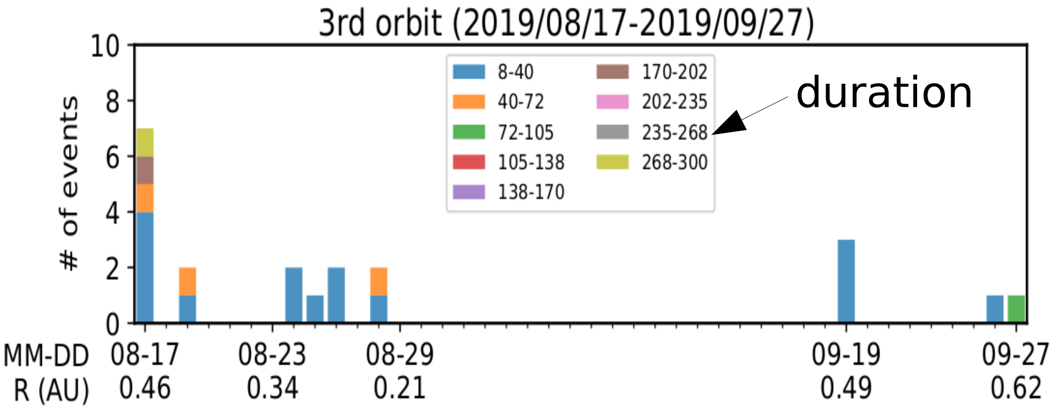

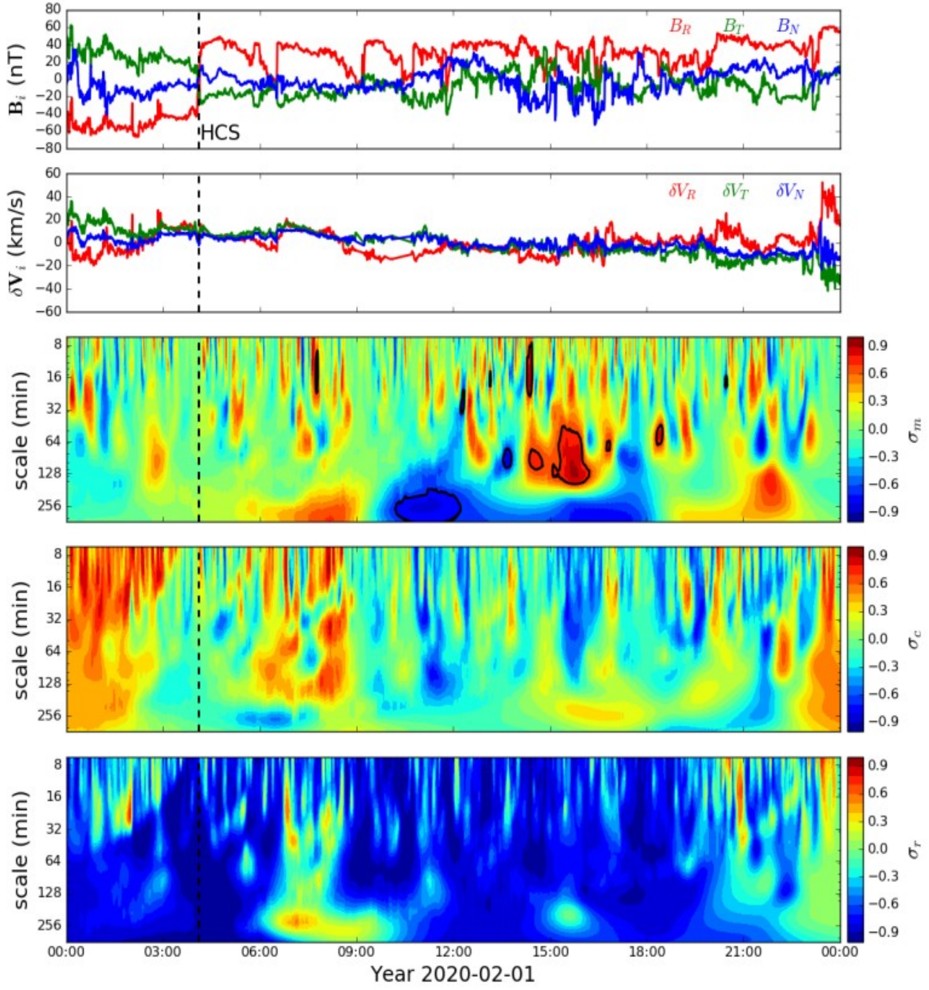

(Zhao et al 2021)

Alfven waves in the solar wind

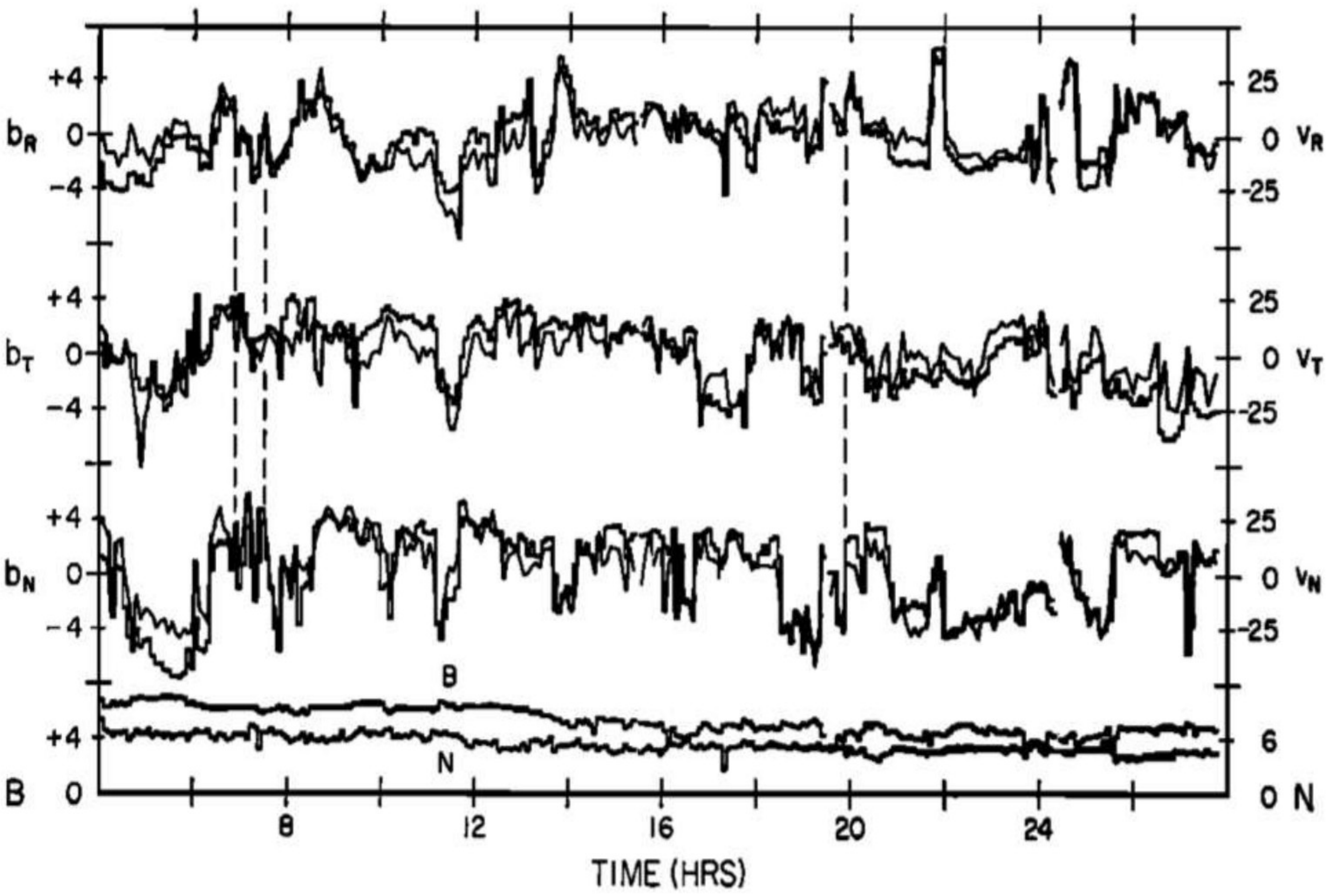

(Belcher & Davis 1971)

Velocity and magnetic field fluctuations are highly correlated.

Pure Alfven wave

Does there exist a turbulence?

Solar wind observation

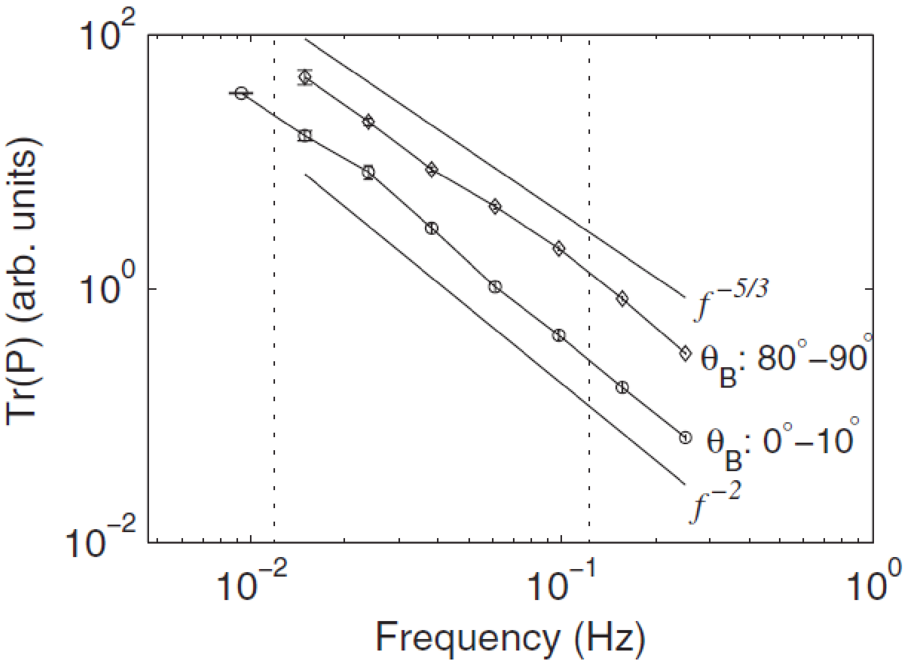

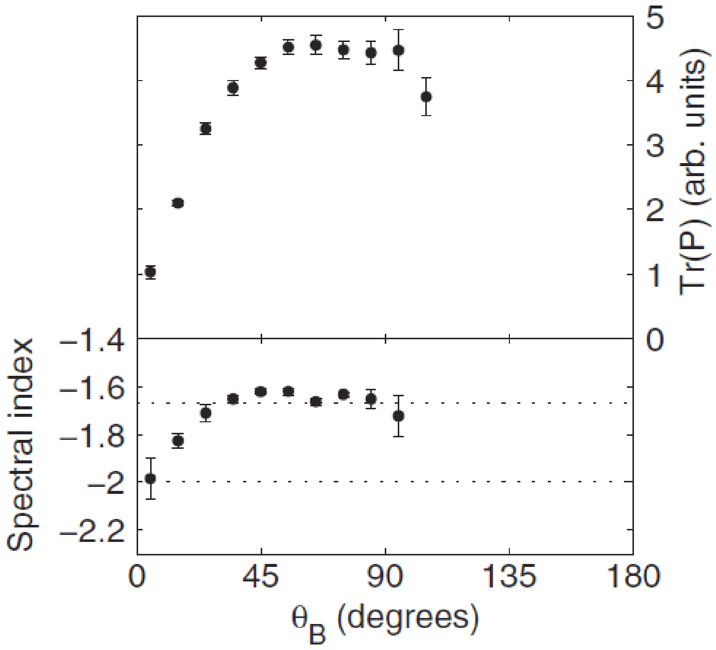

Horbury et al. (2008)

- One of the properties of solar wind turbulence is spectral anisotropy.
- Critical balance predicts different scalings for parallel and perpendicular spectra ${k_\perp}^{-5/3}$ and ${k_\parallel}^{-2}$ provided the (normalized) cross helicity $|\sigma_c|$ ~ 0.
- Assuming Taylor's hypothesis and the Parker spiral magnetic field, PSP is more likely to measure parallel spectra $k_\parallel$ close to the Sun.

Highly field-aligned flow

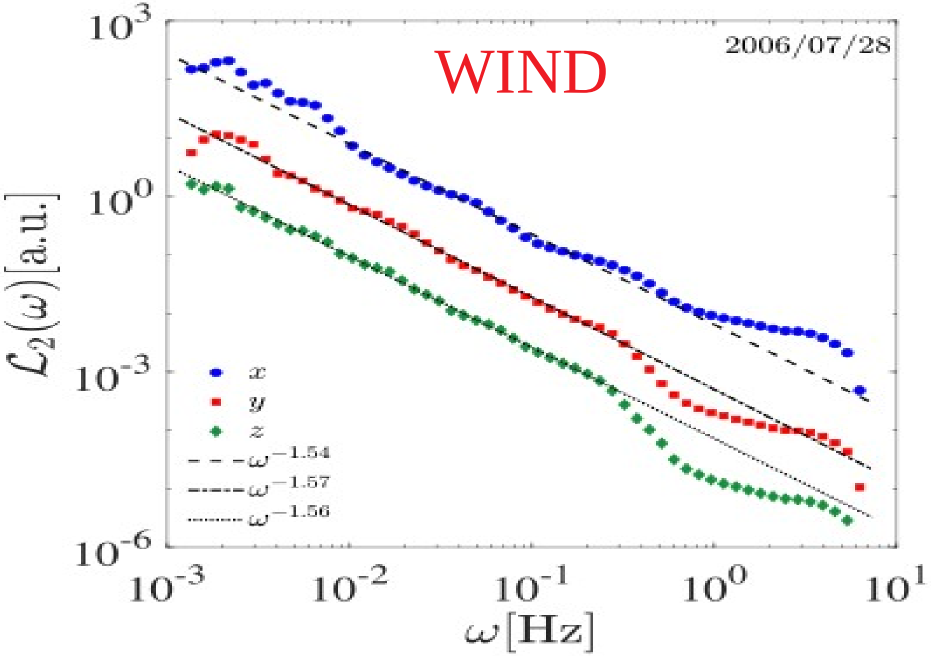

(Telloni et al 2019)

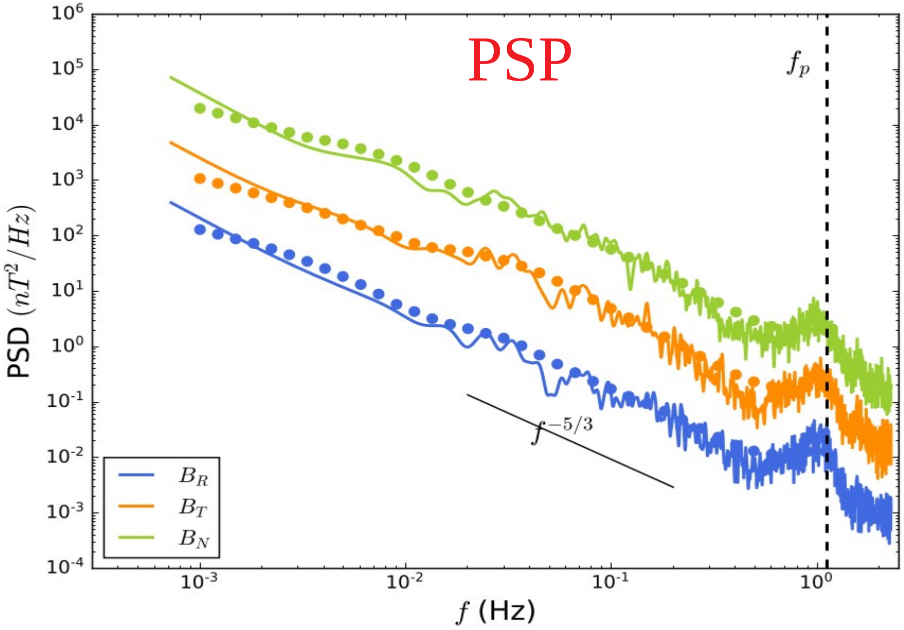

(Zhao et al. 2020)

WIND & PSP observed highly field-aligned flow:

- the normalized cross helicity ~ 0.8 - 1
- the spectra show a -5/3 power law.

- Different from critical balance theory (Goldreich, P. & Sridhar, S. 1995) which predicts a k^{-2} power-law for a field-aligned flows.

Which theory can describe a $k^{-5/3}$ power-law exhibited by a field-aligned flows?

NI MHD 2D + Slab spectral theory

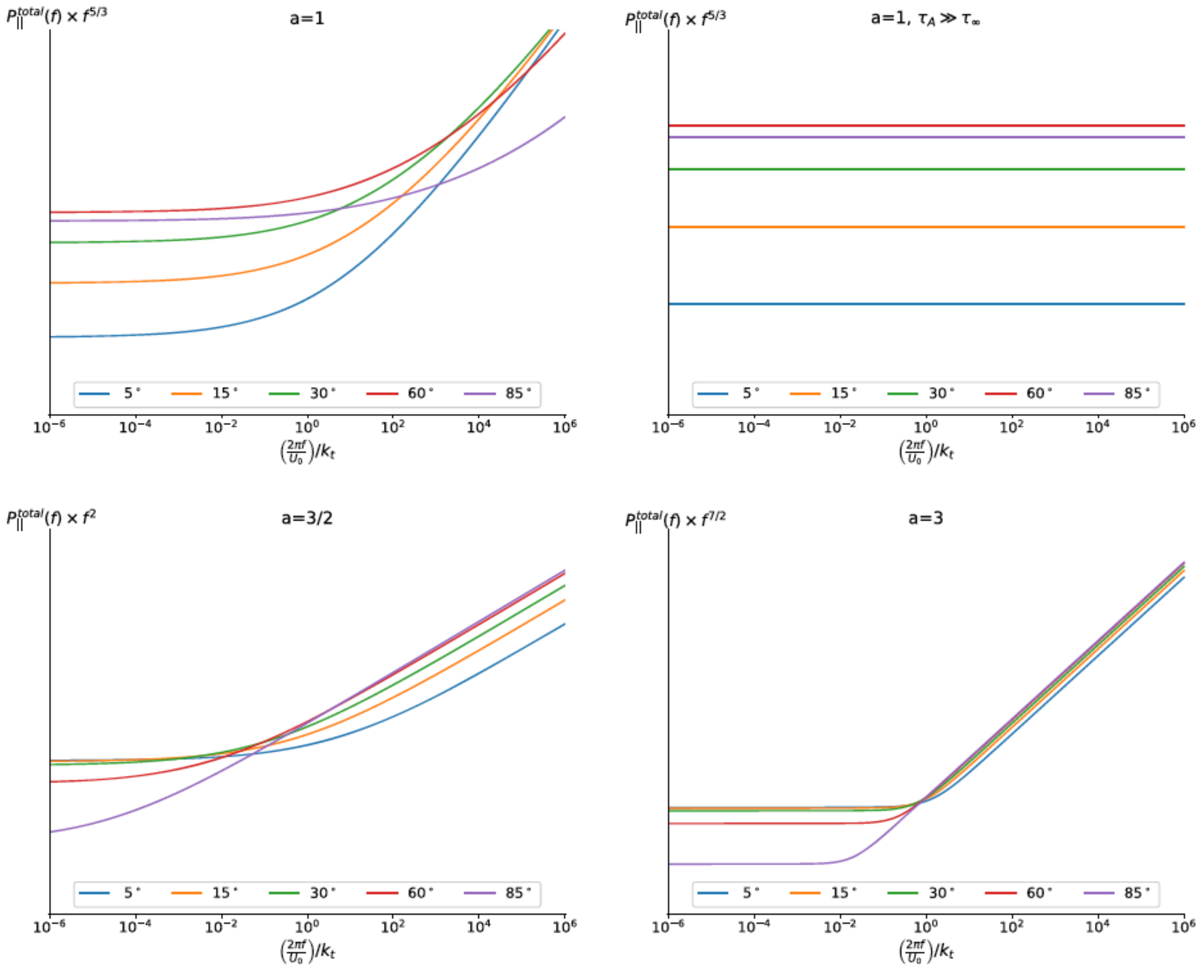

- For strongly imbalanced turbulence, we find

$$G^*(k_\perp) = \varepsilon_*^{1/2}\varepsilon_\infty^{1/6}k_\perp^{-5/3} \quad \text{and}$$
$$G^*(k_z) = \varepsilon_*^{1/2}\varepsilon_\infty^{1/6}k_t^{2(a-1)/3}k_z^{-(2a+3)/3},$$

- The choice $a = 1$ corresponds to a parallel spectral index of -5/3, as we observe in the PSP data.

(Zank et al. 2020)

NI MHD 2D + slab turbulence transport equations

(Zank et al 2017;2018; Adhikari et al 2017; 2020)

Describe the radial evolution of 2D and slab turbulence

NI MHD theory is applicable in solar wind plasma even when the incompressible MHD theory is not applicable.

(Zank & Matthaeus 1991; Zank & Matthaeus 1992, 1993; 2020; Hunana & Zank 2010)

Transport of NI MHD turbulence (Zank et al 2017)

2D

Nonlinear terms

$$\frac{\partial \mathbf{z}^{\infty\pm}}{\partial t} + \mathbf{U}\cdot\nabla\mathbf{z}^{\infty\pm} + \mathbf{z}^{\infty\mp}\cdot\nabla\mathbf{z}^{\infty\pm} + \mathbf{z}^{\infty\mp}\cdot\nabla\mathbf{U} + \frac{\mathbf{z}^{\infty\pm}-\mathbf{z}^{\infty\mp}}{4}\nabla\cdot\mathbf{U} - \frac{\mathbf{z}^{\infty\pm}-\mathbf{z}^{\infty\mp}}{4}\mathbf{z}^{\infty\mp}\frac{1}{\rho}\cdot\nabla\rho = -\frac{1}{\rho}\nabla\left(P^{\infty}+\frac{B^{\infty 2}}{2\mu_0}\right).$$

→ No Alfven wave effect

Slab

Nonlinear terms

$$\frac{\partial \mathbf{z}^{*\pm}}{\partial t} + (\mathbf{U}\mp\mathbf{V}_{A0})\cdot\nabla\mathbf{z}^{*\pm} + \mathbf{z}^{\infty\mp}\cdot\nabla\mathbf{z}^{*\pm} + \mathbf{z}^{*\mp}\cdot\nabla\mathbf{z}^{\infty\pm} + \mathbf{z}^{*\mp}\cdot\nabla\mathbf{z}^{*\pm} + \frac{1}{4}(\mathbf{z}^{*\pm}-\mathbf{z}^{*\mp})\nabla\cdot\mathbf{U}$$
$$+ \mathbf{z}^{*\mp}\cdot\nabla(\mathbf{U}\pm\mathbf{V}_{A0}) \pm \frac{1}{2}\frac{1}{\rho}\mathbf{z}^{*\mp}\cdot\nabla\rho_{sw}\mathbf{V}_{A0} - \frac{1}{4}(\mathbf{z}^{*+}-\mathbf{z}^{*-})\frac{1}{\rho}\mathbf{V}_{A0}\cdot\nabla\rho$$
$$\pm\frac{1}{4}(\mathbf{z}^{\infty+}-\mathbf{z}^{\infty-})\frac{1}{\rho}\mathbf{z}^{*\mp}\cdot\nabla\rho \mp \frac{1}{4}(\mathbf{z}^{*+}-\mathbf{z}^{*-})\frac{1}{\rho}\mathbf{z}^{\infty\pm}\cdot\nabla\rho \mp \frac{1}{2}(\mathbf{z}^{*+}-\mathbf{z}^{*-})\cdot\nabla\mathbf{U}$$
$$= -\frac{1}{\rho}\nabla\left(P^{*}+\frac{1}{\mu_0}\mathbf{B}^{*}\cdot\mathbf{B}+\frac{1}{\mu_0}\mathbf{B}^{*}\cdot\mathbf{B}^{\infty}\right).$$

→ Alfven wave effect

$$\mathbf{z}^{\infty\pm} \equiv \mathbf{u}^{\infty} \pm \frac{\mathbf{B}^{\infty}}{\sqrt{\mu_0\rho(\mathbf{x})}} \equiv \mathbf{u}^{\infty}\pm\mathbf{v}_A^{\infty}, \qquad \mathbf{z}^{*\pm} \equiv \mathbf{u}_1 \pm \frac{\mathbf{B}^{*}}{\sqrt{\mu_0\rho(\mathbf{x})}} \equiv \mathbf{u}_1 \pm \mathbf{v}_A^{*}.$$

NI MHD Turbulence Transport Equation

2D

$$U\frac{dE_T^\infty}{dr} = -\left(\frac{E_T^\infty}{2} + \left(2a - \frac{1}{2}\right)E_D^\infty\right)\frac{dU}{dr} - \frac{2U}{r}\left(\frac{E_T^\infty}{2} + \left(2a - \frac{1}{2}\right)E_D^\infty\right)$$
$$- \frac{U}{\sigma f(r)}\left(\frac{E_T^\infty}{2} + \left(2a - \frac{1}{2}\right)E_D^\infty\right)\exp\left(\frac{r - r_a}{\sigma}\right)\frac{f_m - f(r)}{\exp\left(\frac{r-r_a}{\sigma}\right) + 1}$$
$$- \alpha\frac{|E_T^\infty + E_C^\infty|^2|E_T^\infty - E_C^\infty|^{1/2}}{L_\infty^+} - \alpha\frac{|E_T^\infty - E_C^\infty|^2|E_T^\infty + E_C^\infty|^{1/2}}{L_\infty^+}$$
$$+ \frac{S^{\langle z^{\infty+2}\rangle} + S^{\langle z^{\infty-2}\rangle}}{2};$$

Superradial expansion

Nonlinear term

Turbulence source

NI/slab

$$(U - V_A)\frac{dE_T^*}{dr} = -\frac{1}{2}\frac{dU}{dr}E_T^* + (2b-1)\frac{U}{r}E_T^* + \frac{V_A}{2\rho}\frac{d\rho}{dr}E_T^*$$
$$+ \frac{1}{2}(2b-1)\frac{U}{\sigma f(r)}E_T^*\exp\left(\frac{r - r_a}{\sigma}\right)\frac{f_m - f(r)}{\exp(\frac{r-r_a}{\sigma}) + 1}$$
$$- 2\alpha\frac{E_T^*|E_T^\infty + E_C^\infty||E_T^\infty - E_C^\infty|^{1/2}}{L_\infty^+}$$
$$+ \frac{S^{\langle z^{*+2}\rangle}}{2},$$

(Zank et al 2017, 2018; Adhikari et al 2020,2022, Telloni et al 2022)

Conservation of Turbulence Energy

2D

$$\frac{1}{r^2 f(r)}\frac{d}{dr}\left[r^2 f(r) U(E_w^\infty + P_w^\infty)\right] = U\frac{dP_w^\infty}{dr} + \rho\Big[-\alpha\frac{|E_T^\infty + E_C^\infty|^2 |E_T^\infty - E_C^\infty|^{1/2}}{L_\infty^+} - \alpha\frac{|E_T^\infty - E_C^\infty|^2 |E_T^\infty + E_C^\infty|^{1/2}}{L_\infty^+} + \frac{S^{\langle z^{\infty+2}\rangle} + S^{\langle z^{\infty-2}\rangle}}{2}\Big],$$

Turbulence energy density

$$E_w^\infty = \rho E_T^\infty/2$$

Turbulence pressure

$$P_w^\infty = \frac{\rho}{2}\left[\frac{E_T^\infty}{2} + \left(2a - \frac{1}{2}\right)E_D^\infty\right] = \frac{E_w^\infty}{2}\left[1 + 2\left(2a - \frac{1}{2}\right)\sigma_D^\infty\right]$$

NI/slab

$$\frac{1}{r^2 f(r)}\frac{d}{dr}\left[r^2 f(r)\big((U - V_A)E_w^* + UP_w^*\big)\right] = U\frac{dP_w^*}{dr} + 2E_w^*\left(4b\frac{u}{r} + 2b\frac{U}{f(r)}\frac{df(r)}{dr}\right) + \frac{\rho}{2}\Big[-2\alpha\frac{E_T^*|E_T^\infty + E_C^\infty||E_T^\infty - E_C^\infty|^{1/2}}{L_\infty^+} + \frac{S^{\langle z^{*+2}\rangle}}{2}\Big],$$

Turbulence energy density

$$E_w^* = \rho E_T^*/2$$

Turbulence pressure

$$P_w^* = E_w^*/2$$

(Adhikari et al 2022, see also Wang et al. 2022)

The Astrophysical Journal, 929:98 (14pp), 2022 April 10 https://doi.org/10.3847/1538-4357/ac5cc3

Possible Evidence for Shear-driven Kelvin–Helmholtz Instability along the Boundary of Fast and Slow Solar Wind in the Corona

Daniele Telloni[1], Laxman Adhikari[2], Gary P. Zank[2,3], Lingling Zhao[2], Luca Sorriso-Valvo[4,5], Ester Antonucci[1], Silvio Giordano[1], and Salvatore Mancuso[1]

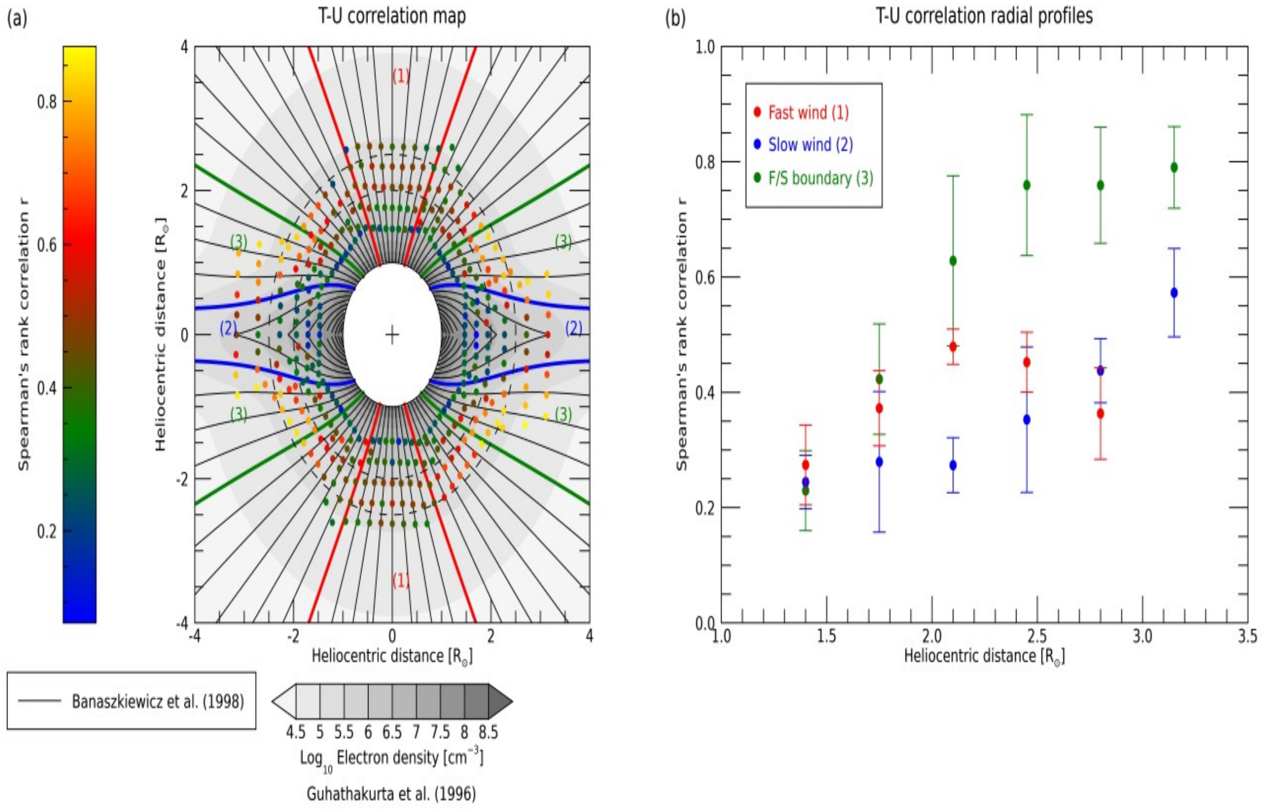

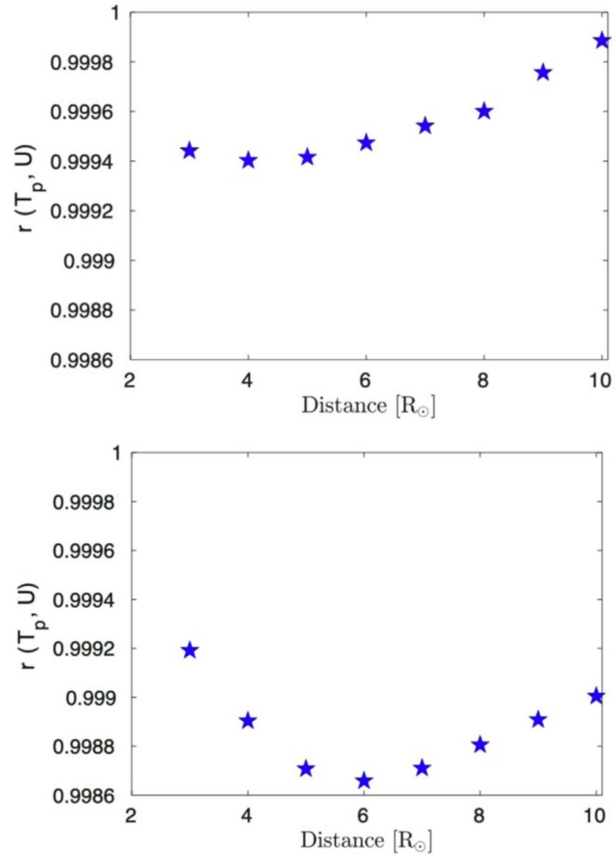

Model results + Fast solar wind

Model results + PSP data

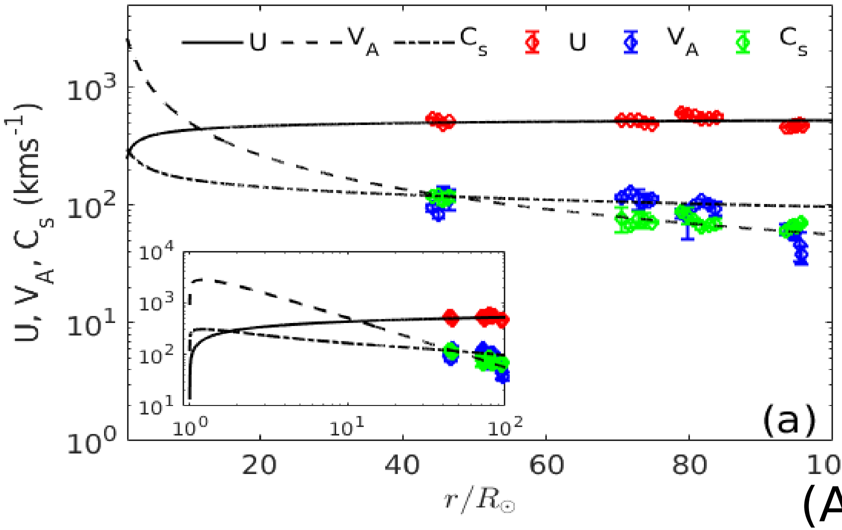

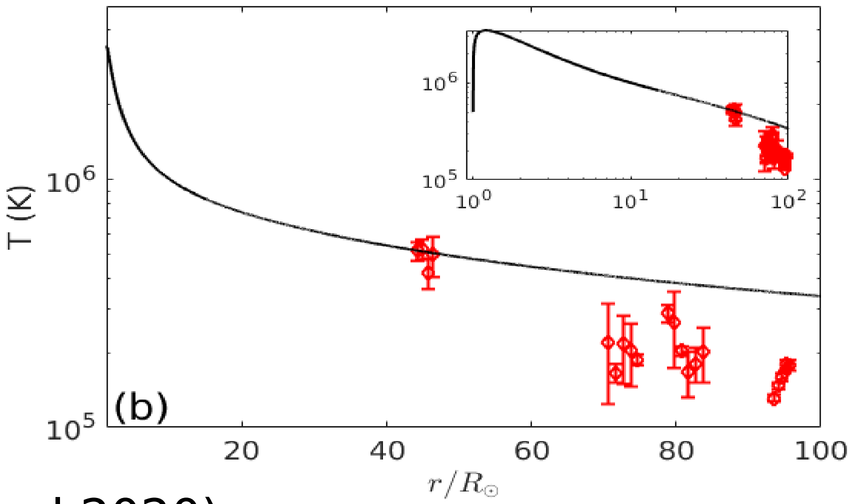

(Adhikari et al 2020)

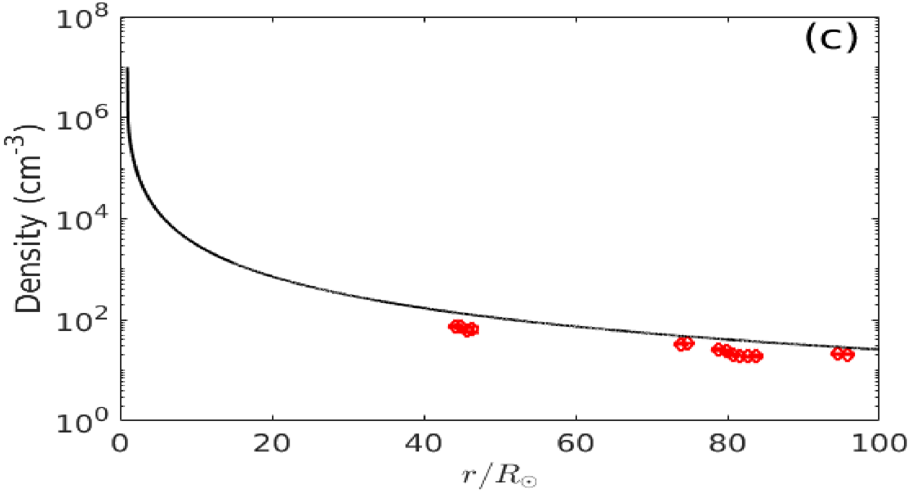

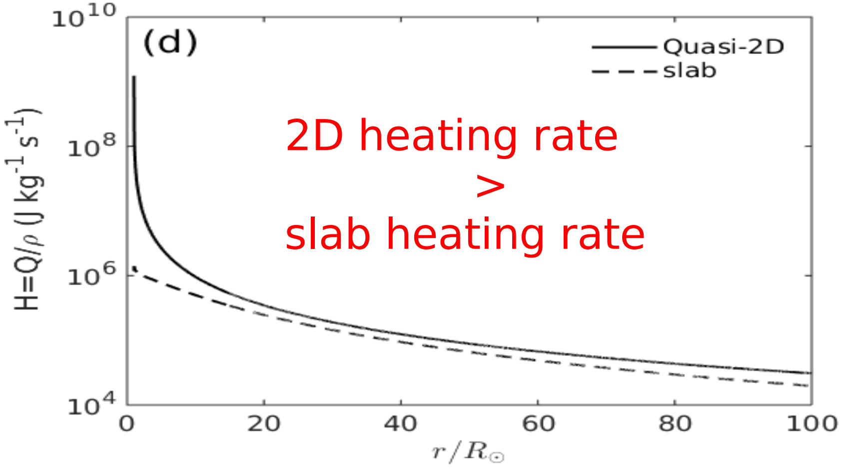

Model results + PSP data

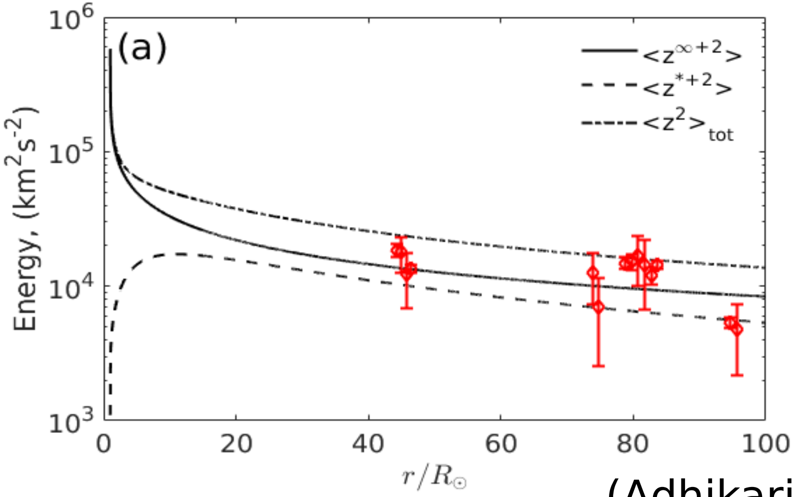

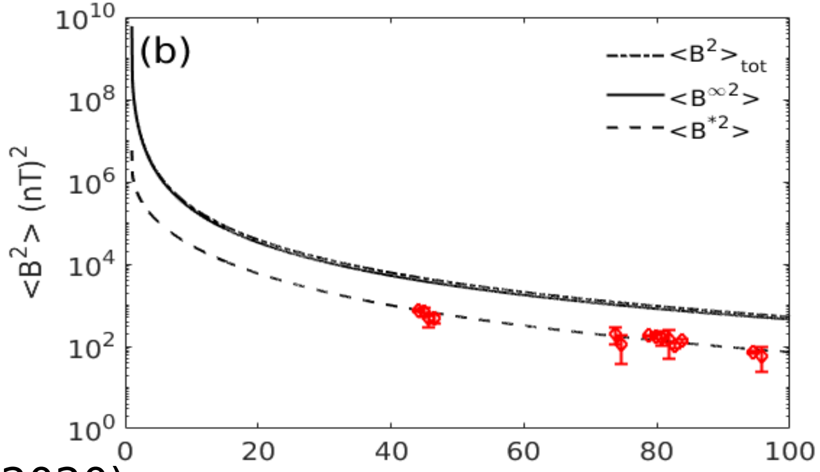

(Adhikari et al 2020)

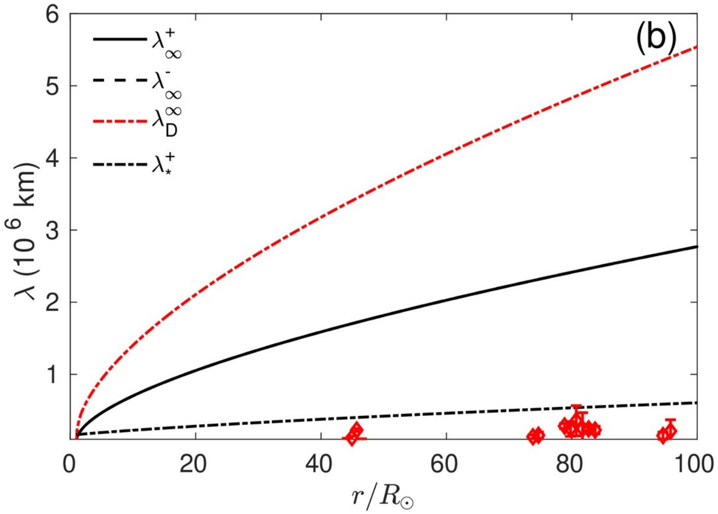

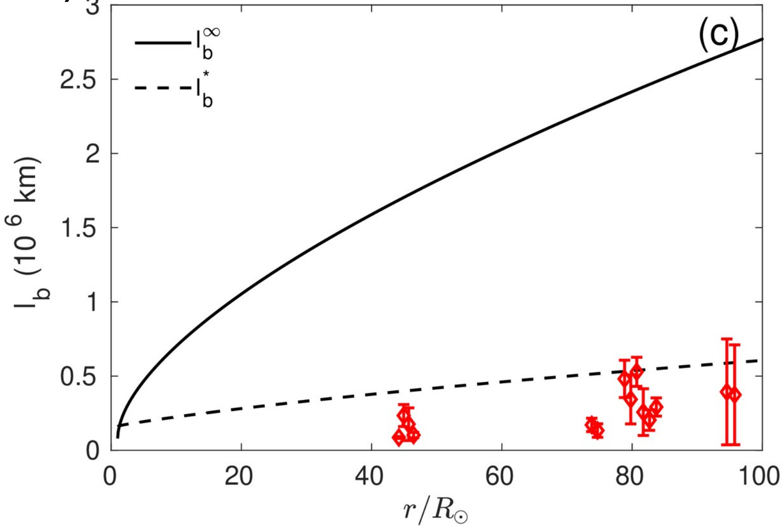

Model results + PSP & Helios 2 data

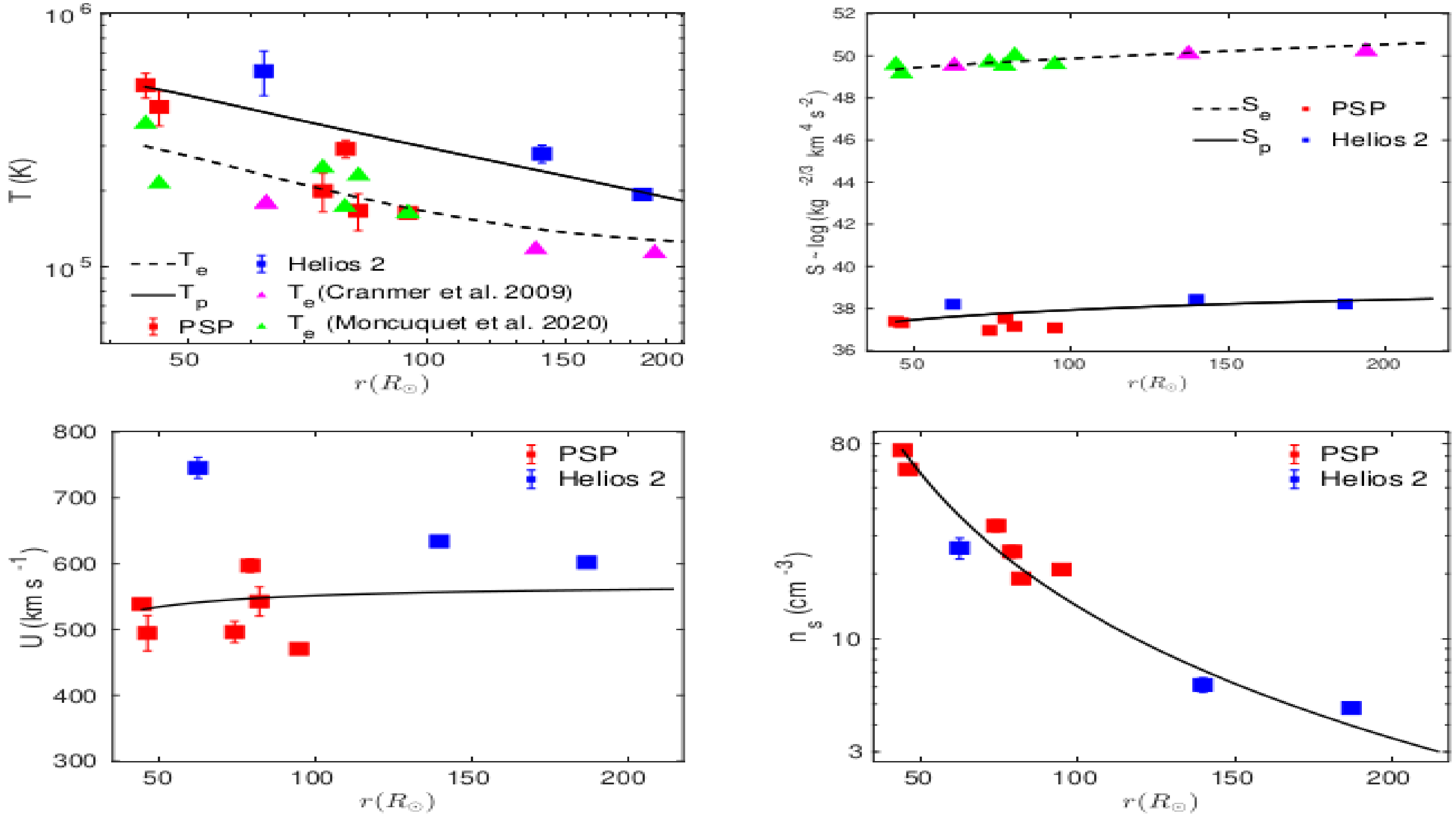

Electron's effect is included.

(Adhikari et al 2021)

Model results + Slow solar wind

First Parker Solar Probe–Solar Orbiter Radial Alignment

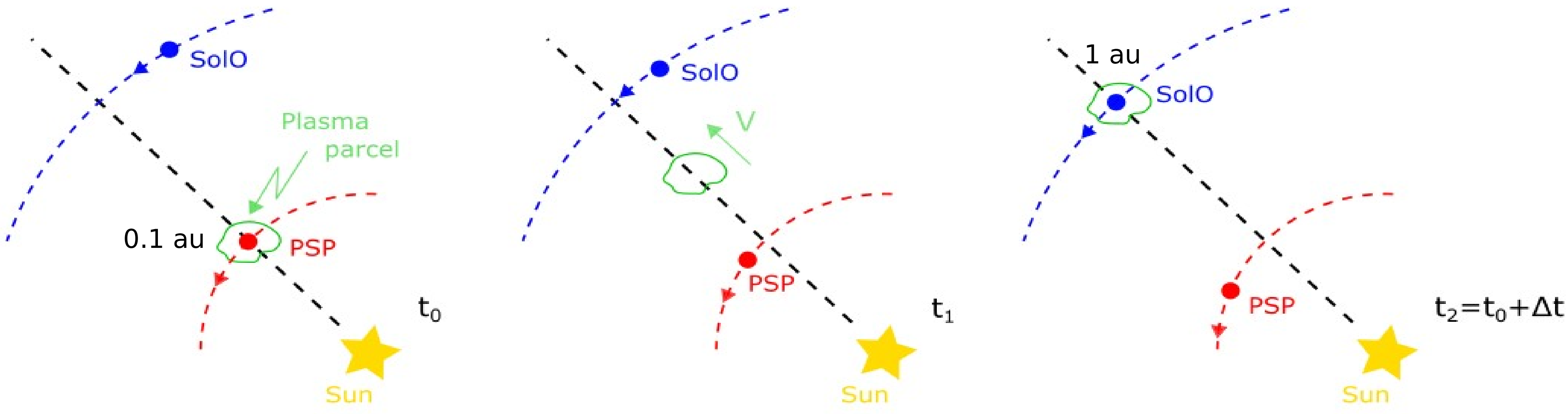

- The identification of the time intervals corresponding to the same plasma parcel observed at PSP and SolO distances during their radial alignment with the Sun is based on the ballistic approach.

(Telloni et al 2021)

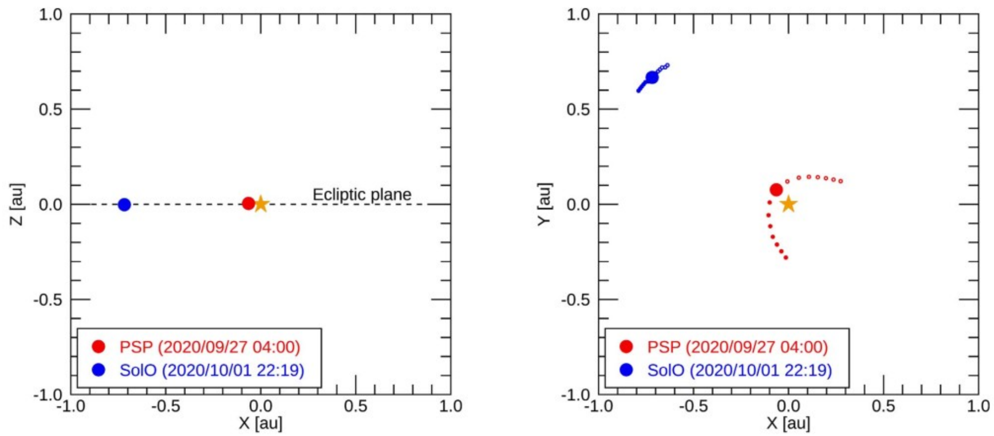

Evolution of Slow Solar Wind

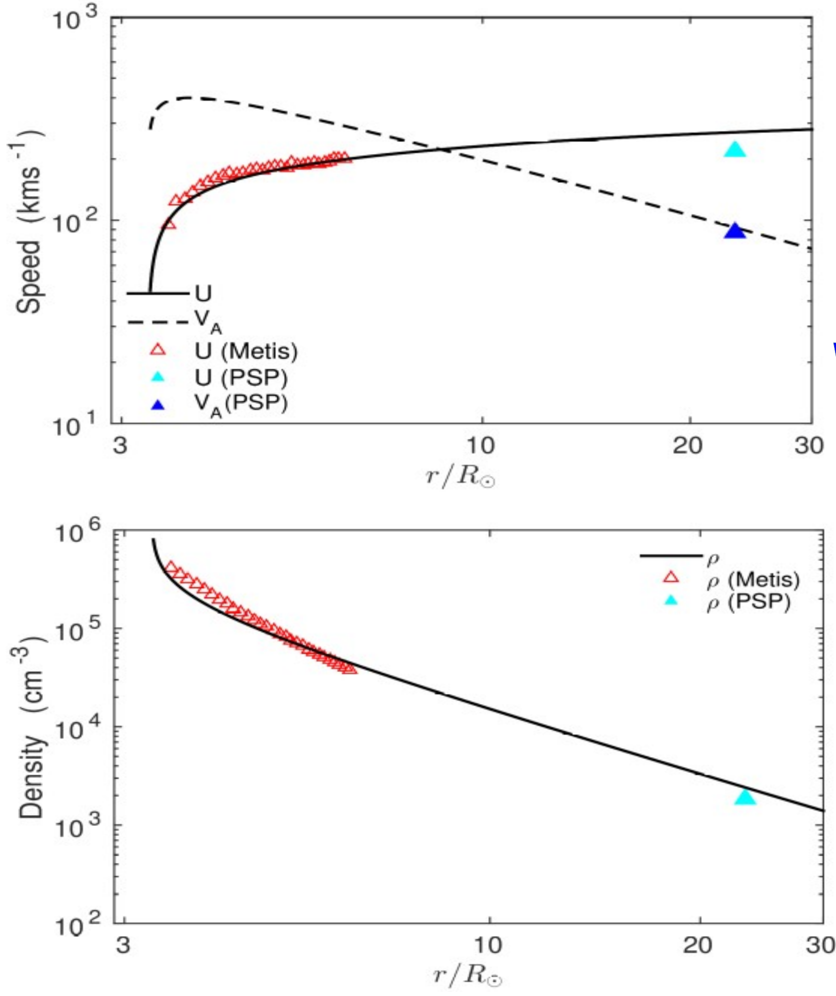

(Adhikari et al 2022)

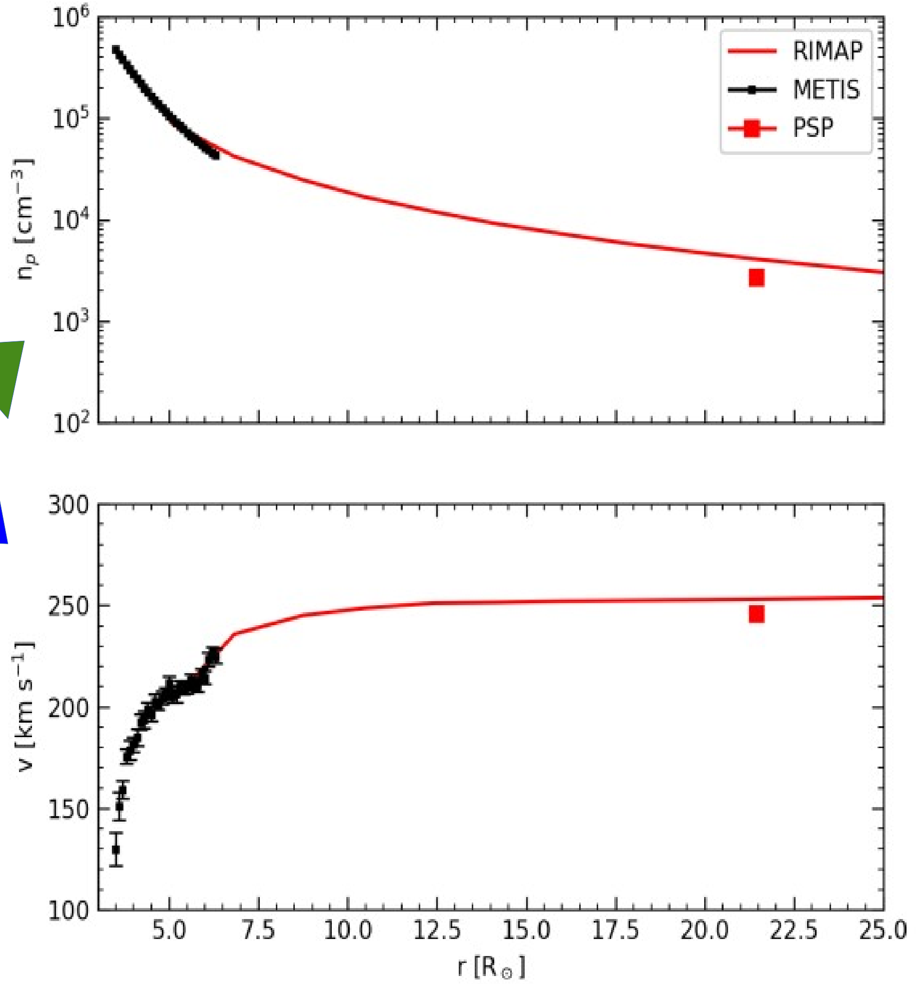

(Biondo et al 2022)

Evolution of Turbulence Energy

(Adhikari et al 2022)

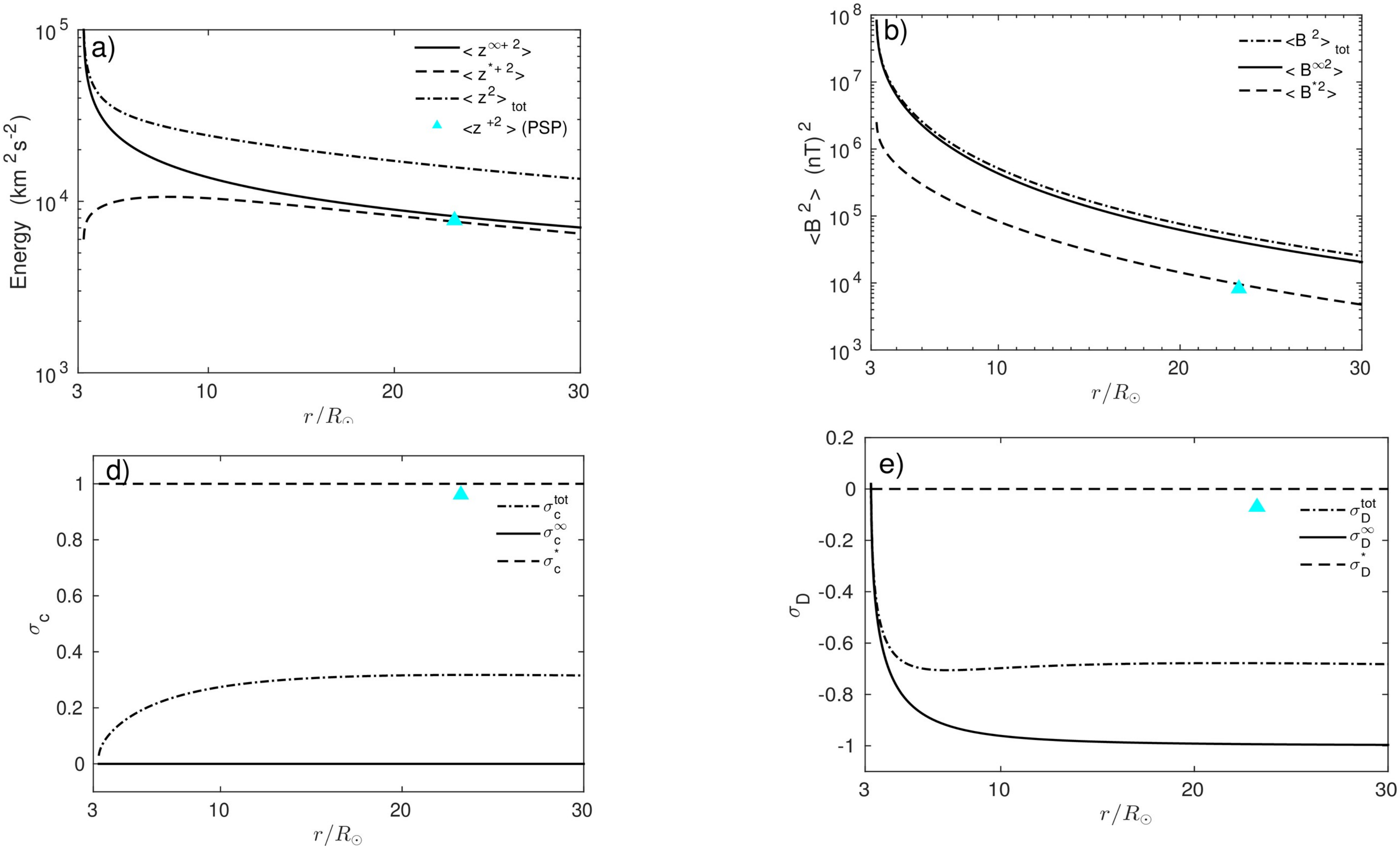

Evolution of Correlation Length

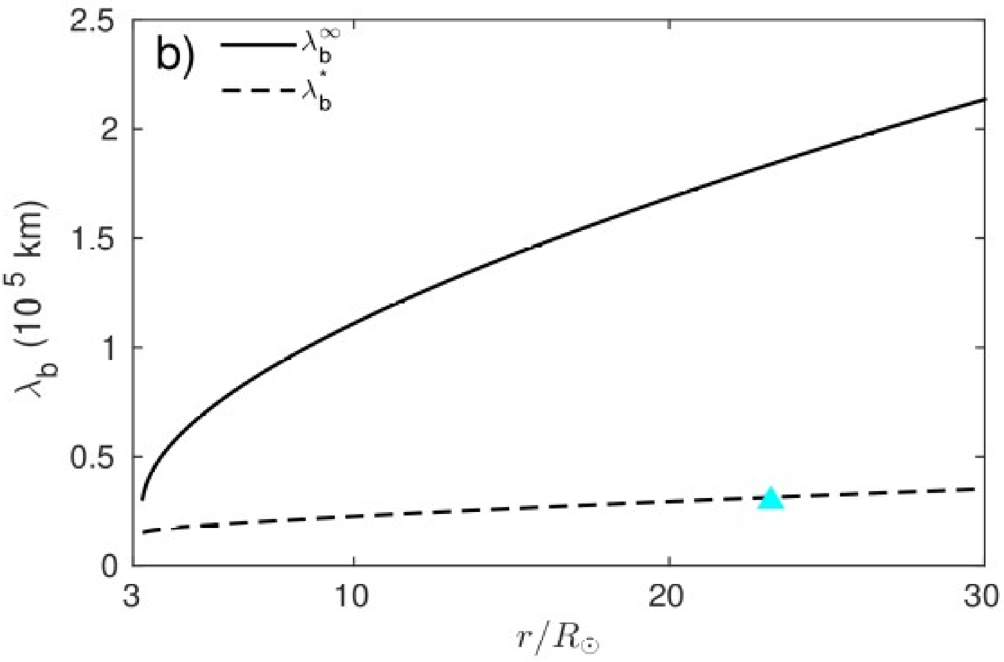

(Adhikari et al 2022)

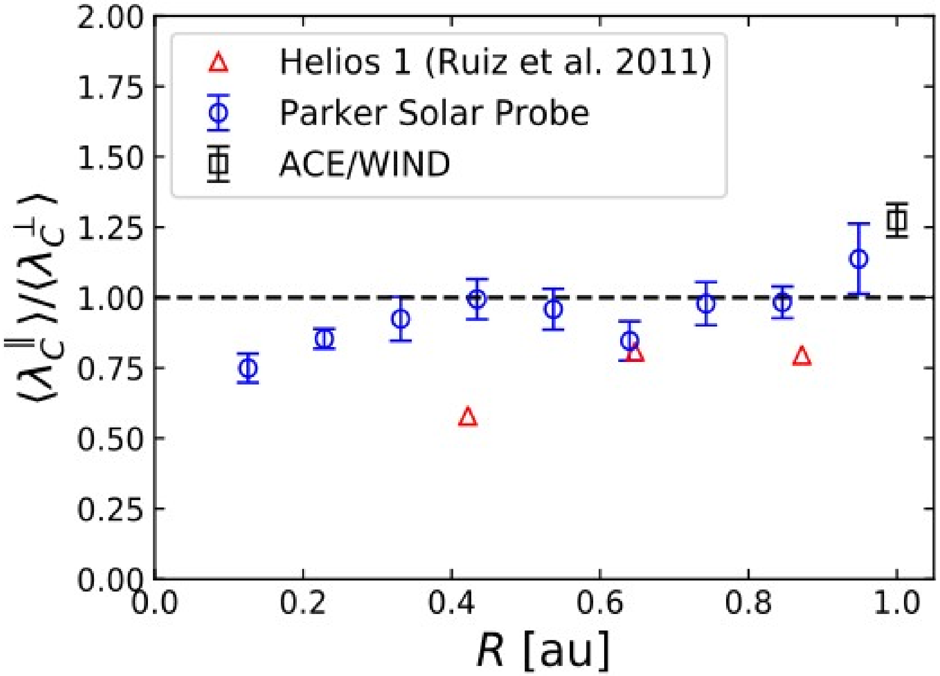

(Cuesta et al 2022)

The theoretical 2D correlation length (solid curves) increases much more rapidly than the theoretical NI/slab correlation length. This is different from Ruiz et al. (2011) and Cuesta et al. (2022). In their results, the slab (or parallel) correlation length increases faster than the 2D (or perpendicular) correlation length.

Turbulence energy vs Angle

Slab

$$f\,P_{SUM}(f) = 2\,C_S\left(\frac{2\pi f}{V_w \cos\psi}\right)^{1-q} + 2\,C_2\left(\frac{2\pi f}{V_w \sin\psi}\right)^{1-q}$$

2D

(Bieber et al 1996)

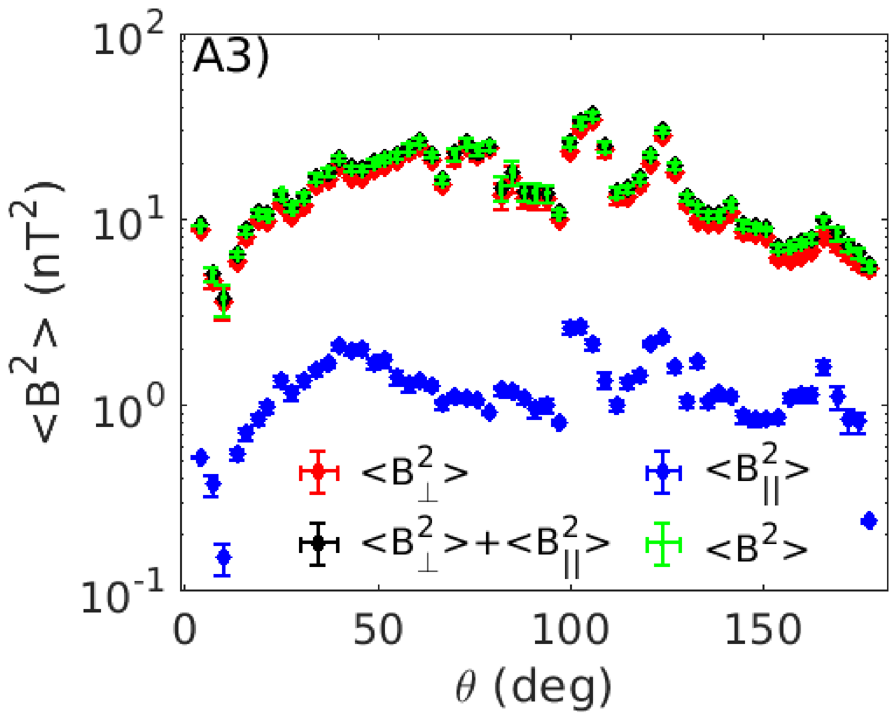

(Adhikari et al 2021)

2D and slab turbulence energy

(Adhikari et al 2022)

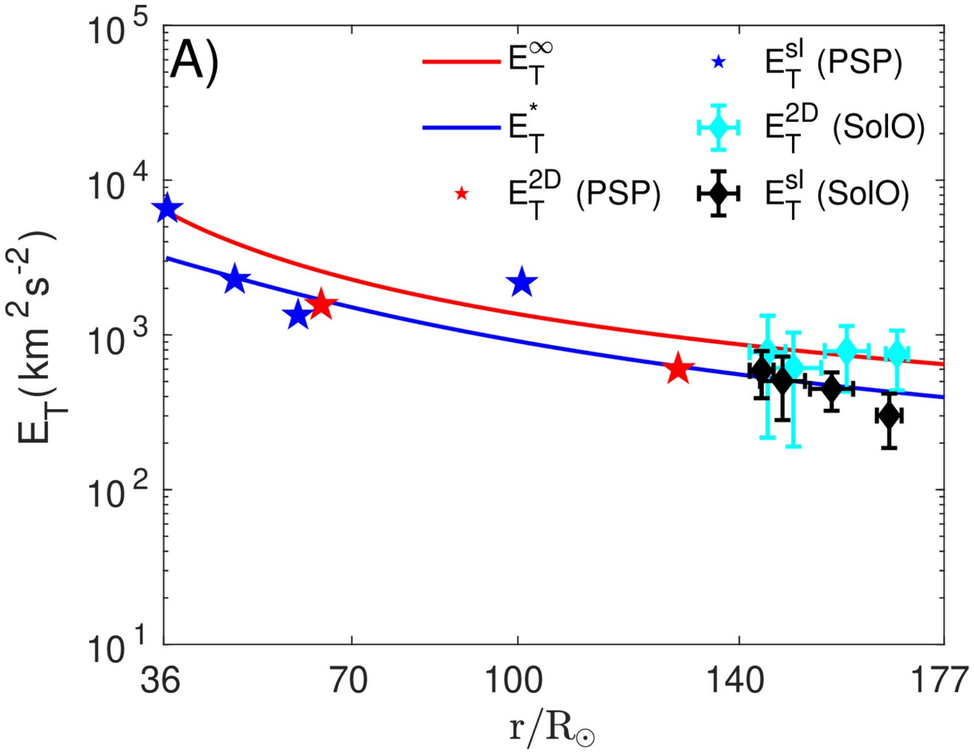

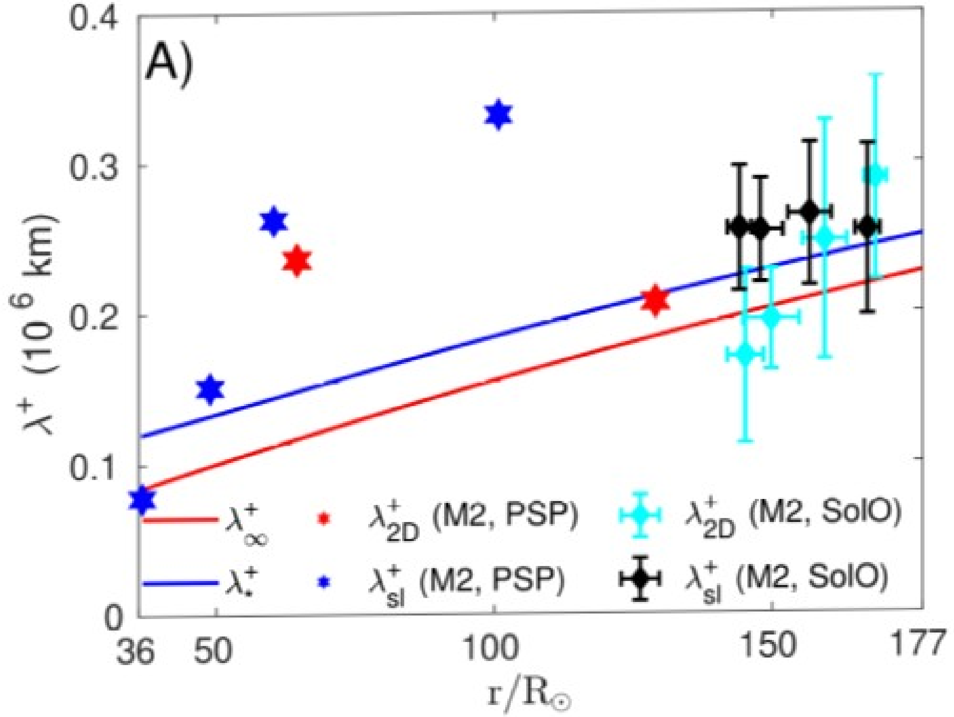

i) $0° < \theta_{UB} < 25°$ and $155° < \theta_{UB} < 180°$, and ii) $65° < \theta_{UB} < 115°$

Slab turbulence — 2D turbulence

2D and slab cascade rate

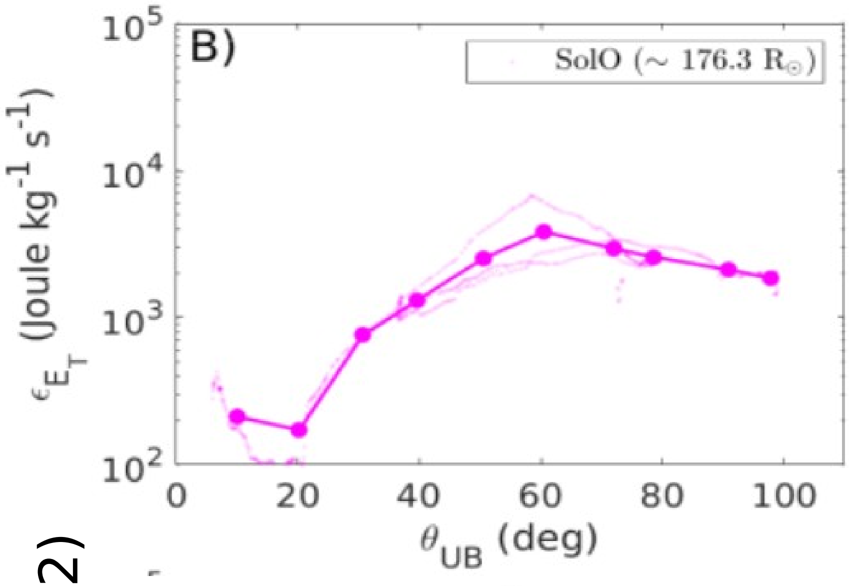

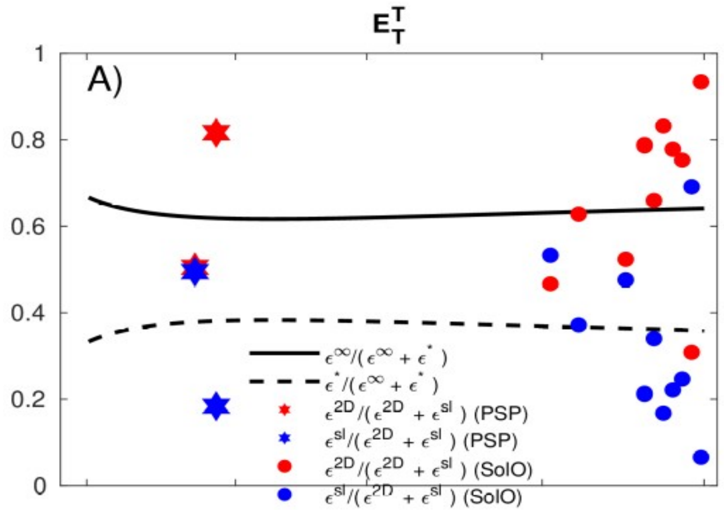

(Adhikari et al 2022)

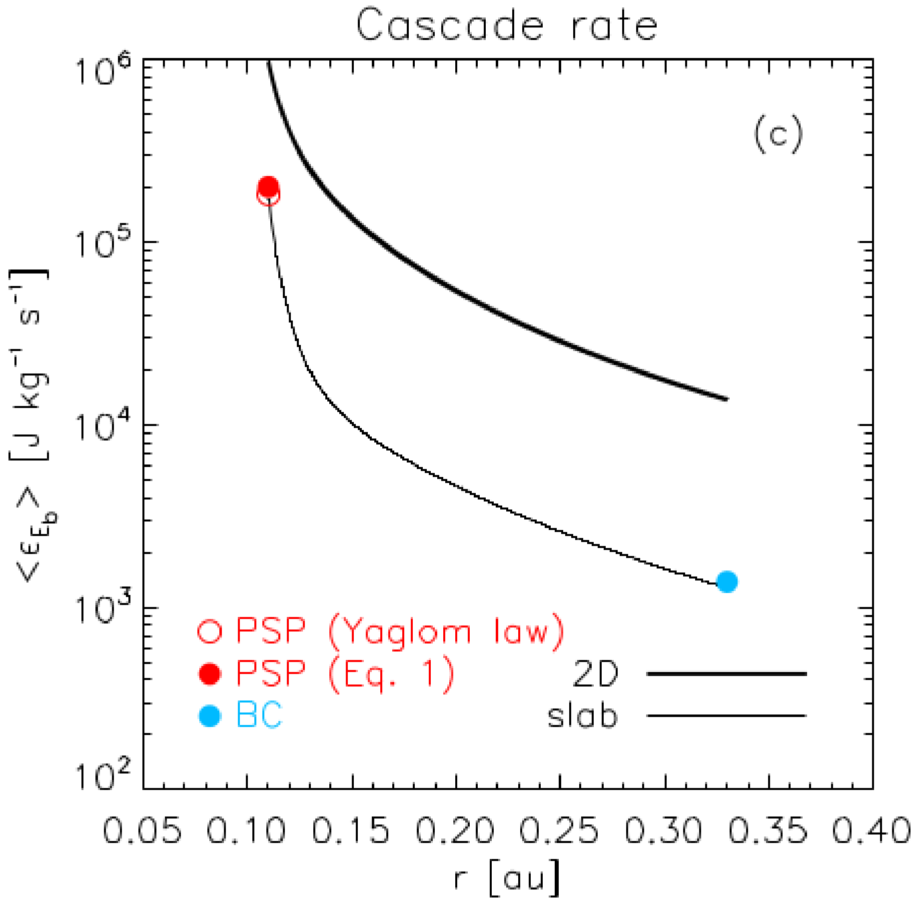

(Telloni et al 2022)

Summary

- Dissipation of 2D turbulence is mainly responsible for the heating of the solar corona and the acceleration of the solar wind.
- PSP (and Helios) observations of large-scale SW and turbulence quantities consistent with NI/slab results from quasi-2D model since the fast wind observations made in the fast field-aligned solar wind flow (only slab fluctuations visible to PSP).
- PSP observations of large-scale Alfvenic slow SW and turbulence quantities consistent with NI/slab results.
- Near the Sun, PSP observes mainly the slab component. Whereas, SolO observes both the 2D and slab components frequently.
- 2D turbulence energy/heating rate is larger than the slab turbulence energy/heating rate.